Journal of Controlled Release 288 (2018) 1–13

Contents lists available at ScienceDirect

Journal of Controlled Release

journal homepage: www.elsevier.com/locate/jconrel

Hyaluronic acid-endostatin2-alft1 (HA-ES2-AF) nanoparticle-like conjugate for the target treatment of diseases

Feng Sun[a,b,1], Yang Yu[a,b,c,1], Zhifang Yang[a,b,1], Zhendong Wang[a,b], Yan Li[a,b], Fengshan Wang[a,d], Haining Tan[a,b,d,*]

[a] National Glycoengineering Research Centre, Shandong University, Jinan 250012, Shandong, PR China
[b] Shandong Provincial Key Laboratory of Carbohydrate chemistry and Glycobiology, Shandong University, Jinan, 250012, Shandong, PR China
[c] Institute of Advanced Medical Sciences, Shandong University, Jinan 250012, Shandong, PR, China
[d] School of Pharmaceutical Sciences, Shandong University, Jinan, 250012, Shandong, PR China

ARTICLE INFO

Keywords:
ES2-AF
Chemical modification
Anti-angiogenesis
Targeting
Half-life

ABSTRACT

Anti-flt1 peptide (GNQWFI, AF) specifically binds to Vascular Endothelial Growth Factor Receptor 1 (VEGFR1), thereby inhibiting the interaction of VEGFR1 with a series of ligands. ES2 (IVRRADRAAVP) can effectively inhibit the proliferation and invasion of endothelial cells and play a key role in anti-angiogenesis. AF and ES2 peptides differ in their activity. To better exploit the advantages of both, we designed a new peptide called ES2-AF (IVRRADRAAVPGGGGGGNQWFI). Hyaluronic acid (HA) is widely used in the pharmaceutical industry because of its biodegradable and high load performance. The HA-specific cell surface receptor CD44 was highly expressed in the tumour site during the anti-tumour study. Therefore, we used HA as a modifier to chemically modify ES2-AF; it was expected that the modified compound would have preferable solubility, stronger targeting, longer half-life, and better anti-angiogenesis effects *in vivo*. In this study, the anti-proliferative, anti-migration and targeting activities of HA-ES2-AF *in vitro* were studied by MTT, ELISA, transwell and SPR assays. Meanwhile, the anti-neovascularization activity of HA-ES2-AF *in vivo* was studied by CAM assay, and the targeting of HA-ES2-AF to tumour tissue was studied by bioimaging techniques. Finally, we also studied the half-life of HA-ES2-AF *in vivo*. In short, the bioactivity of the new peptide ES2-AF was enhanced to a certain extent, and ES2-AF modified by HA had higher anti-neovascularization activity *in vitro* and *in vivo*, had stronger targeting to tumour tissue, and had a significantly prolonged half-life *in vivo*. These results laid the foundation for its further development into targeting anti-tumour drugs.

1. Introduction

Neonatal vessels provide nutrients for solid tumour growth and metastasis; therefore, many drugs are used to inhibit neovascularization in order to achieve the goal of inhibiting tumour growth [1]. Endostatin (ES) is the most potent endogenous neovascular inhibitor [2,3], and it has been found that the active sequence ES2 (IVRRADRAAVP), which plays a key role in anti-angiogenesis, is a fragment of 11 amino acids from its amino terminal [4]. ES2 can effectively inhibit the proliferation and invasion of endothelial cells, and its inhibition of angiogenesis activity is approximately 3 times that of the complete ES sequence [5–7]. ES2 also plays an important role in the treatment of diseases caused by diabetic eye disease, rheumatoid arthritis and other neovascularization [8,9]. However, ES2 has many shortcomings as a protein and peptide drug, such as short half-life and poor stability *in vivo*, which limits its extensive clinical application [10].

AF peptide (GNQWFI) is a VEGFR1-selective hexapeptide, selected from the Position Scanning Synthetic Peptide Library, which specifically binds to VEGF, thereby inhibiting the interaction of VEGF with a series of ligands. It can effectively inhibit VEGF and VEGF / PDGF-induced endothelial cell migration and tube formation. AF can be easily synthesized at a lower production cost, but its poor water solubility hindered its clinical application [11–13]. Chemical modification has opened up a new way to develop protein and peptide drugs [14]. Polyethylene glycol (PEG) is a commonly used modifier to improve medical proteins. It can prolong half-life *in vivo*, reduce or eliminate the immunogenicity of proteins and increase stability to enhance drug application potential [15]. However, PEG also has shortcomings; the most

* Corresponding author.
E-mail address: hainingtan@sdu.edu.cn (H. Tan).
[1] These authors contributed equally to this work.

https://doi.org/10.1016/j.jconrel.2018.08.038
Received 31 May 2018; Received in revised form 16 August 2018; Accepted 28 August 2018
Available online 29 August 2018

significant limitation is that it is non-biodegradable, and some recent studies on anti-PEG antibodies have raised new concerns [16,17].

Hyaluronic acid (HA) is a negatively charged, non-sulphated linear glycosaminoglycan found in bovine vitreous that binds specifically to CD44 [13,18]. It has been found that macromolecule HA (> 106 kDa) could inhibit the proliferation and invasion of endothelial cells [19,20]. In recent years, HA and its derivatives have been widely used clinically due to its safety, targeting, good biocompatibility and other biological functions and unique physical and chemical properties. In terms of drug delivery, HA can be used not only as a carrier for peptide and protein drugs but also as a targeting agent to deliver these drugs or even other drug carriers to the tumour and other lesions [21]. In this study, the ES2-AF peptide was first synthesized and then chemically modified with HA (Mw 240 kDa) in order to target tissue, inhibit neovascularization and migration and achieve the purpose of inhibiting tumour growth. Nuclear magnetic resonance (^{1}H NMR), methyl thiazolyl tetrazolium (MTT) assay, cell migration assay, tube formation assay, ELISA test, chicken chorioallantoic membrane (CAM) assay, surface plasmon resonance (SPR), bioimaging assay, and pharmacokinetic studies were all used in this study.

2. Materials and methods

2.1. Materials

Synthetic short peptides AF, ES2 and AF-ES2 were purchased from China Peptides Co., Ltd. (Shanghai, China). Hyaluronic acid, average molecular weight 240 kDa) was kindly supplied by Freda Group (Jinan, China). EAhy926 endothelial cells (ATCC Number: CRL-2922) were obtained from Shanghai Cell Bank, the Institute of Cell Biology, China Academy of Sciences (Shanghai, China). Phosphate buffer saline (PBS), fibronectin (FN), trypsin, methylthiazolyldiphenyl-tetrazolium bromide (MTT), and bovine serum albumin (BSA) were all purchased from Solarbio Science & Technology Co., Ltd. (Shanghai, China). Dulbecco's modified Eagle medium (DMEM) was purchased from Gibco®, Life Technologies (Carlsbad, CA, USA). Foetal bovine serum (FBS) was purchased from Hangzhou Sijiqing Biological Engineering Co., Ltd. (Hangzhou, China). Matrigel matrix, transwell chambers, 96-well plates, 24-well plates, 25-mL cell culture bottles and 15-mL centrifuge tubes were purchased from Corning INC. (New York, NY, USA). Leucocrystal violet was purchased from Sigma-Aldrich (St. Louis, MO, USA). Dimethyl sulphoxide (DMSO), methanol, acetic acid glacial and tetrabutylammonium hydroxide (TBA) were purchased from Sinopharm Chemical Reagent Co., Ltd. (Shanghai, China). Benzotriazol-1-yloxytris(dimethylamino)-phosphonium hexafluorophosphate (BOP) was purchased from TCI Co., Ltd. (Shanghai, China). Fluorescein isothiocyanate (FITC) was purchased from Shanghai Purple One Reagent Factory (Shanghai, China). Vascular endothelial growth factor$_{165}$ (VEGF$_{165}$) and basic fibroblast growth factor (bFGF) were purchased from Peprotech (Rocky Hill, NJ, USA). Tween 20 and TMB colour liquid were purchased from Beyotime Biological Technology Co., Ltd. (Shanghai, China). Anti-human IgG-HRP-Fc was purchased from Cusabio Biological Engineering Co., Ltd. (Wuhan, China). Recombinant CD44 protein and Flt-Fc were purchased from R & D Systems (Minneapolis, MN, USA). All other chemicals and reagents were of the highest commercial grade available.

2.2. Synthesis of the HA-ES2-AF conjugate

HA-TBA was synthesized according to a previously established method [22]. Briefly, HA was dissolved in water, and Dowex 50 W ion-exchange resin was added to the solution (resin:HA = 3:1). After exchanging for 6 h, the resin was filtered using a 0.45-μm filter, and the filtrate was titrated by TBA-OH to pH 7.0. The resulting solution was then lyophilized. The obtained HA-TBA was dissolved in DMSO; then, 2.5 M excess of BOP was added to activated carboxyl groups of HA-TBA with 30 min mixing after dissolving completely. ES2-AF peptide and an equimolar amount of DIPEA were added to the HA-TBA solution and mixed at 37 °C. After 24 h, an equal volume of 1 M NaCl aqueous solution was mixed with the reaction solution. The pH of the mixture was adjusted to 7.0 by dropwise addition of 1 M NaOH solution. The resulting product was dialyzed against a large amount of 0.3 M NaOH solution, 25% ethanol and water, and then lyophilized for 3 days [11,23].

2.3. Cell culture

Cell experiments were conducted using endothelial EAhy926 cells. The media and operation specifications for cell culture were in accordance with the previous study [24]. EAhy926 cells were cultured in DMEM medium with 10% FBS and maintained under a 5% CO_2 atmosphere at 37 °C.

2.4. Cell proliferation assay

MTT assay was used to determine the anti-proliferative effects of HA-ES2-AF on endothelial cells. EAhy926 cells were seeded into 96-well plates (6×10^3 cells/well). After incubation overnight, endothelial cells were treated with AF, ES2, ES2-AF, HA & ES2-AF, and HA-ES2-AF at peptide concentrations of 25 μg/mL, 150 μg/mL, 400 μg/mL, 600 μg/mL and 800 μg/mL (concentrations of 25 μg/mL, 150 μg/mL, 400 μg/mL, 600 μg/mL and 800 μg/mL pointed to the ES2-AF part only) for 48 h. Then, 20 μL MTT reagent was added to each well and further cultured for 4 h under dark conditions. Afterwards, 150 μL dimethyl sulphoxide was added to each well to dissolve the formazan crystal after removing the medium. The absorbance was measured at 490 nm [7,25–27].

2.5. Invasion assay

Invasion assays were performed using the transwell method [7,28,29]. Matrigel was diluted in serum-free DMEM (dilution ratio 1:6) and 50 μL was coated onto each transwell chamber and incubated at 37 °C for 1 h. Then, EAhy926 cells were resuspended in serum-free DMEM and seeded at a density of 5×10^4 cells per chamber. AF, ES2, ES2-AF, the mixture of HA & ES2-AF and HA-ES2-AF were added into transwell chambers at different peptide concentrations of 25 μg/mL, 75 μg/mL and 125 μg/mL (concentrations of 25 μg/mL, 75 μg/mL, 125 μg/mL pointed to the ES2-AF part only). DMEM with 10% FBS was added to the bottom of a 24-well plate, while the chambers were placed in a 24-well plate and incubated at 37 °C for 24 h. Then, the medium was aspirated, and the chambers were washed with PBS. The transwell chambers were placed in a pre-cooled methanol-acetic acid mixture (3:1, 500 μL) for 30 min, stained with 0.1% crystal violet for 30 min, washed three times with PBS and dried. An inverted fluorescence microscope was using to photograph the chambers, and the number of invaded cells was counted.

2.6. Tube formation assay

The tube formation assay was used to evaluate the effect of drugs on endothelial cell tubulogenesis [29,30]. Briefly, Matrigel was pre-melted at 4 °C, coated on 96-well plates (50 μL/well), and then incubated at 37 °C for 30 min for polymerization. EAhy926 cells were seeded in the Matrigel-coated plates (5×10^4 cells/well). Different peptide concentrations (25 μg/mL, 75 μg/mL and 125 μg/mL, concentrations of 25 μg/mL, 75 μg/mL, 125 μg/mL pointed to the ES2-AF part only) of AF, ES2, ES2-AF, the mixture of HA & ES2-AF and HA-ES2-AF were added to each well, and bFGF was added to a final concentration of 5 ng/mL. After incubation at 37 °C for 8 h, the formation of tubular structures of endothelial cells was observed with an inverted fluorescence microscope.

2.7. ELISA assay

$VEGF_{165}$ was dissolved in PBS at a concentration of 0.5 μg/mL and coated onto 96-well plates. After storage at 4 °C overnight, the $VEGF_{165}$-coated 96-well plates were prepared. The plates were washed thrice by PBS and then blocked with 3 wt% BSA at room temperature for 2 h. After washing thrice with PBS, different final peptide concentrations (5 μg/mL, 25 μg/mL, 50 μg/mL, 100 μg/mL and 200 μg/mL, concentrations of 5 μg/mL, 25 μg/mL, 50 μg/mL, 100 μg/mL and 200 μg/mL pointed to the ES2-AF part only) of AF, ES2, ES2-AF, the mixture of HA & ES2-AF, HA-ES2-AF and 500 ng/mL Flt-Fc in 1 wt% BSA were added to the pre-coated wells and maintained for 1 h at room temperature. The 500 ng/mL Flt-Fc without peptide was used as a positive control. PBS with 0.05 wt% Tween 20 was prepared for washing the 96-well plates and anti-human IgG-HRP-Fc in 0.3 wt% BSA (1:1000) was added with 1 h maintaining. After washing twice using PBS with 0.05 wt% Tween 20 and once with PBS alone, the 96-well plates were dried and measured with the TMB method to evaluate the amount of bound Flt-Fc [11,28].

2.8. CAM assay

Chick embryonic chorioallantoic membrane assay was employed to evaluate the anti-angiogenesis effect *in vivo*. Fertilized eggs were maintained at 37 °C and 70% humidity, and after 7 days a small window (0.3–0.4 cm^2) was opened on the top of the eggs. This window formed a new air chamber, which exposed the chick embryonic chorioallantoic membrane. With continued incubation for 48 h, the window was expanded (1 cm^2) and a 5 mm diameter gelatin sponge with different agents was implanted. Eggs were treated with 10 μL bFGF (5 ng/mL) and 20 μL AF, ES2, ES2-AF, HA & ES2-AF, and HA-ES2-AF at peptide concentrations of 5 μg/mL, 25 μg/mL, 50 μg/mL (concentrations of 5 μg/mL, 25 μg/mL, 50 μg/mL pointed to the ES2-AF part only) for another 48 h. Saline was used as blank control [30,31]. The neovascular areas were observed and photographed by a stereomicroscope, and then each group of photographed areas of the same area was analysed by IPP software. The ratio of neovascular area to total area was compared to determine the anti-angiogenic capacity of the drug.

2.9. Pharmacokinetic study

Eight female Wistar rats at a mean weight of 250 g were randomly divided into two groups. Then, 1 mL of ES2-AF or HA-ES2-AF was respectively injected through the femoral vein at a peptide dose of 25 mg/kg (concentration of 25 mg/kg pointed to the ES2-AF part only). Blood samples were collected through the jugular vein at 5 min, 15 min, 30 min, 1 h, 2 h, 6 h, 12 h, 24 h, and 48 h after administration. The collected blood was stored at 4 °C for 2 h and then centrifuged for 10 min at 10,000 rpm to obtain the plasma samples. Plasma samples were precipitated by acetonitrile and the supernatants were collected by centrifugation at 16,000 rpm and 4 °C for 10 min [11,29,32]. Finally, the fluorescence intensity in the samples was measured by fluorescence spectrophotometer (excitation at 280 nm and emission at 350 nm).

2.10. Surface plasmon resonance (SPR) assay

We bound CD44 to a CM5 sensor chip to determine the affinity of HA, HA-ES2-AF and ES2-AF using a Biacore T200 system. First, we performed a pH-scouting process with the pH value range of 3.8–5.0 and discovered that the most suitable pH was 3.8. The sensor chip was activated with EDC/NHS; then, CD44 was immobilized on the surfaces of CM5 chips in sodium acetate buffer pH 3.8. The dissociative carboxyl groups of the chip were blocked by ethanolamine-HCl. The series of concentrations of HA solution as positive controls were flowed across the chip using primary Kinetics/Affinity methods at a flow rate of 30 μL/min. The obtained sensorgrams were analysed to obtain dynamic parameters, including k_D (equilibrium dissociation constant), k_a (binding constant), and k_d (dissociation constant) [33–36]. The other two analytes, HA-ES2-AF and ES2-AF, were analysed in the same way.

2.11. Bioimaging of FITC-labelled HA-ES2-AF conjugate

To study the targeting properties, the modified product and ES2-AF were labelled with FITC following a previous protocol [25]. ES2-AF and HA-ES2-AF were separately dissolved in PBS, and the peptide concentrations were both 1 mg/mL. The two samples were dialyzed in carbonate buffer solution, pH 9–9.5. FITC was dissolved in DMSO (1 mg FITC / 1 mL DMSO). According to FITC: peptide = 1: 1 drop of the FITC-DMSO solution was added to the dialyzed samples and stirred at 4 °C for 4 h. Then, 5 mol/L NH_4CI solution was added to a final concentration of 50 mmol/L with stirring at 4 °C for 2 h. FITC-labelled ES2-AF and HA-ES2-AF were dialyzed in PBS at a low temperature to remove the unlabelled FITC. Preparation and storage were performed at low temperature in the dark. The tumour model was established by subcutaneous injection of 1.0×10^6 B16 cells into the right armpit of each nude mouse. When the tumour volume reached approximately 200 mm^3, the nude mice were injected with FITC-labelled ES2-AF, HA-ES2-AF and HA&HA-ES2-AF *via* tail vein injection. The peptide dose was 50 mg/kg (concentration of 50 mg/kg pointed to the ES2-AF part only). The IVIS kinetics system was used to visualize the mice at 2 h, 4 h, 8 h, 12 h, and 24 h after administration [27,32,37].

2.12. In vivo antitumor efficacy

Nude mice bearing B16 tumors were used to evaluate the therapeutic efficacy of ES2-AF and its derivatives on inhibition of tumour growth. The mice were subcutaneously injected at the right axillary space with 0.1 mL of cell suspension containing 1×10^7 cells. When the tumour tissue grew to 100–200 mm^3, the mice were randomly assigned to one of the three treatment groups ($n = 5$ for each group). The mice of each group were treated every day with the different drugs as described in the following: normal saline (NS; iv.), ES2-AF solution (20 mg/kg; iv.) and HA-ES2-AF solution (60 mg/kg; iv.).

All of the mice were treated for 14 days. The body weights and tumour volumes were recorded every day. The tumour volumes were measured with a vernier caliper, the length is the longest dimension and width is the widest dimension. At day 14, the mice were sacrificed and tumors from each group were surgically excised, rinsed with NS, wiped, weighed and photographed.

2.13. Cell affinity assay

The affinity activity of HA-ES2-AF to endothelial cells was determined. Fluorescein 6-isothiocyanate (FITC)-labelled-ES2-AF, HA-ES2-AF and HA&HA-ES2-AF were respectively incubated with endothelial cells (30×10^4 cells/well) for 4 h at 37 °C. Fluorescent labeling methods have been described in previously published articles [25]. The concentrations of all groups were set to be 0.5 μg/mL, 1 μg/mL, 2 μg/mL, 5 μg/mL, 10 μg/mL and 25 μg/mL (concentrations were pointed to the ES2-AF part only). After incubation, the cells were detached with 0.25% trypsin/EDTA and washed three times with precooled PBS. The cell pellet was then resuspended in 0.5 mL of PBS. Fluorescence-activated cell sorting analysis was performed using FlowJo.

3. Results and discussion

3.1. Characterization of the HA-ES2-AF conjugate

It has been reported that macromolecule HA (> 106 kDa) has anti-angiogenesis effect, so we choose hyaluronic acid with molecular weight of 240 kDa to modify ES2-AF. To ensure the dissolubility of HA

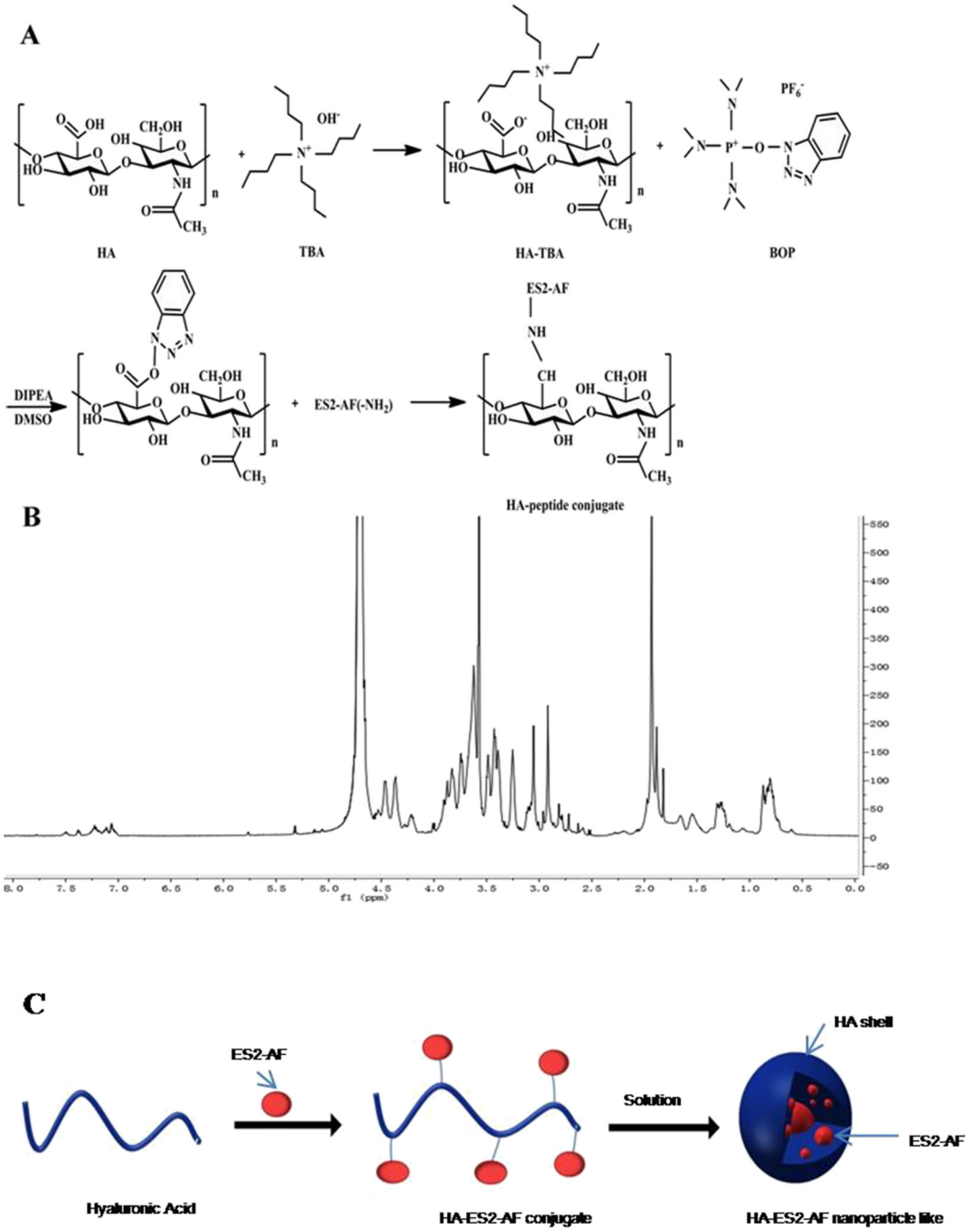

Fig. 1. (A) Synthetic route for HA-ES2-AF. (B) ^{1}H NMR spectrum of HA-ES2-AF. (C) Schematic illustration of HA-ES2-AF conjugates.

in DMSO, HA-TBA was prepared using ion-exchange resin by an ion-exchange method. As shown in Fig. 1(A), when the carboxyl of HA was activated with BOP, the ES2-AF peptide was conjugated with HA by the formation of an amide linkage between the amino group of the ES2-AF peptide and the activated carboxyl of HA. As shown in Fig. 1(B), the successful conjugation of HA-ES2-AF was characterized by ^{1}H NMR spectrogram. From the obtained spectra, peaks at 7.10–7.65 ppm corresponded to the aromatic rings of phenylalanine and tryptophan, and peaks at 1.85–1.95 ppm correspond to the methyl resonance of the acetamido moiety of HA. By comparing peaks at 1.85–1.95 ppm and peaks at 7.10–7.65 ppm, we determined the peptide content. The successful conjugation of HA and the novel angiogenic peptide ES2-AF was confirmed by ^{1}H NMR spectroscopy, and the prepared ES2-AF contained 60 peptide molecules per HA chain.

Conjugating macromolecular polymers with drugs has been applied as a promising platform for drug delivery [38]. Synthetic polymers exhibit high thermal and chemical stabilities and can be synthesized with controlled molecular weight and low dispersity [39]. In this study, the conjugation of hydrophobic ES2-AF to HA may result in the formation of self-assembled nanoparticles/micelle-like structures (as shown in Fig. 1 C), in which drugs can be physically encapsulated [40]. Thus, better stability, bioactivity and longer half-life *in vivo* can be expected.

3.2. Cell proliferation assay

The effect of ES2-AF and HA-ES2-AF on the proliferation of EAhy926 cells was assessed by MTT assay. First, we investigated the anti-proliferation ability of AF, ES2 and AF-EF2. As shown in Fig. 2, at the concentrations of 25 μg/mL, 150 μg/mL, 400 μg/mL, 600 μg/mL,

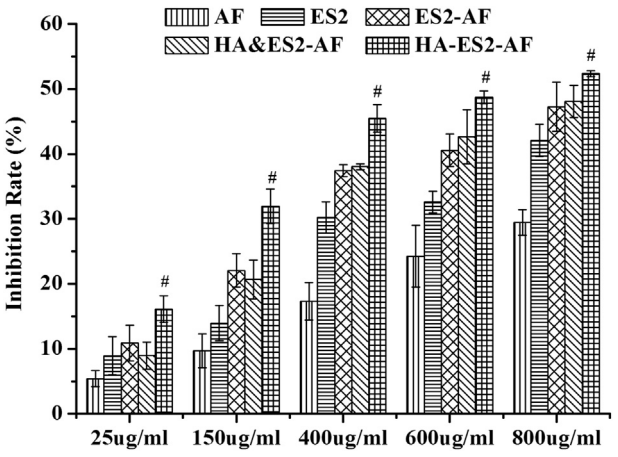

Fig. 2. Inhibition of ES2-AF and HA-ES2-AF on endothelial cell proliferation *in vitro*. Data represent the means ± SD ($n = 5$). $^{\#}P < .05$, significantly different compared with the ES2-AF or HA & ES2-AF group.

and 800 μg/mL, the inhibitory rates of AF, ES2 and ES2-AF were (5.42 ± 1.21)%, (9.72 ± 2.61)%, (17.32 ± 2.89)%, (24.24 ± 4.76)%, and (29.46 ± 1.98)%; (8.94 ± 2.94)%, (13.96 ± 2.73)%, (30.24 ± 2.41)%, (32.6 ± 1.66)%, (42.1 ± 2.46)% and (10.9 ± 2.76)%, (22.06 ± 2.57)%, (37.42 ± 0.90)%, (40.56 ± 2.53)%, and (47.26 ± 3.78)%, respectively. At the same concentrations, the inhibitory rates of HA & ES2-AF and HA-ES2-AF were (8.96 ± 2.10)%, (20.68 ± 2.99)%, (38.05 ± 0.46)%, (42.67 ± 4.17)%, and (48.06 ± 2.47)%, and (16.12 ± 2.03)%, (31.95 ± 2.63)%, (45.48 ± 2.09)%, (48.71 ± 1.00)% and (52.36 ± 0.47)%, respectively. As seen from the above results, the inhibition rate increased in a dose-dependent manner as the concentration increased in all groups. However, the results showed that when the concentration exceeded 150 μg/mL, the inhibitory effect of mixture group on endothelial cell proliferation was stronger than ES2-AF group. According to the literature, high molecular weight HA can inhibit the proliferation of endothelial cells when the concentration is more than 100μg/mL [41], so when the concentration exceed 150μg/mL, the HA and peptide in the mixture also play a role in inhibiting the proliferation of endothelial cells, so there is a tendency for the mixed group to inhibit endothelial cell proliferation slightly stronger than ES2-AF group. The new synthetic peptide, ES2-AF, retained or even improved the ability of ES2 to

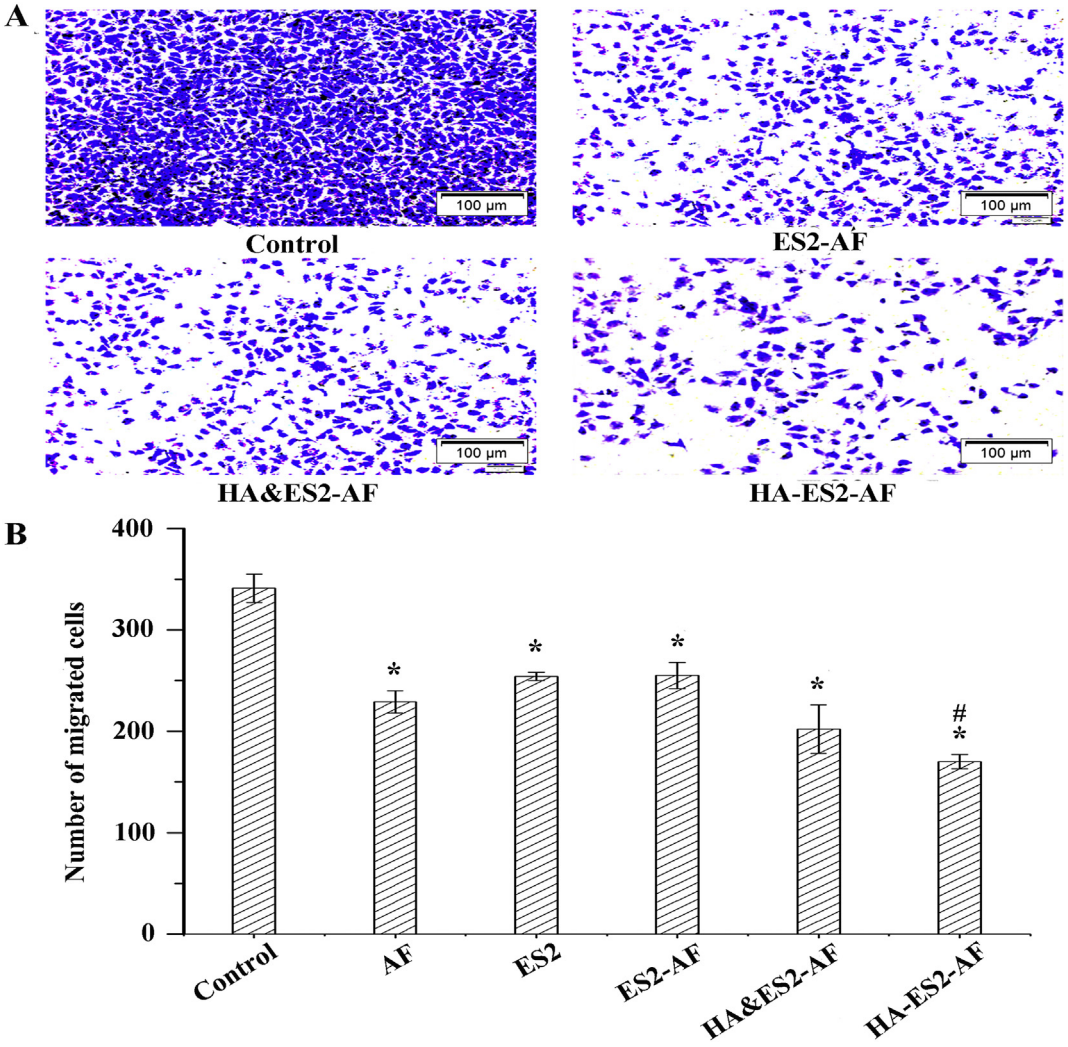

Fig. 3. Conjugation of HA to ES2-AF enhanced the inhibition of the transwell invasion of endothelial cells. (A) Inhibition of the transwell invasion of endothelial cells after incubation with AF, ES2, ES2-AF, HA-ES2-AF and the mixture of HA & ES2-AF at the concentration of 200 μg/mL. (B) Comparison of invaded cell numbers for AF, ES2, ES2-AF, HA-ES2-AF and the mixture of HA & ES2-AF in the transwell invasion assay. Data represent means ± SD ($n = 5$). $^{*}P < .05$, significantly different compared with the control group. $^{\#}P < .05$, significantly different compared with the ES2-AF or HA & ES2-AF group.

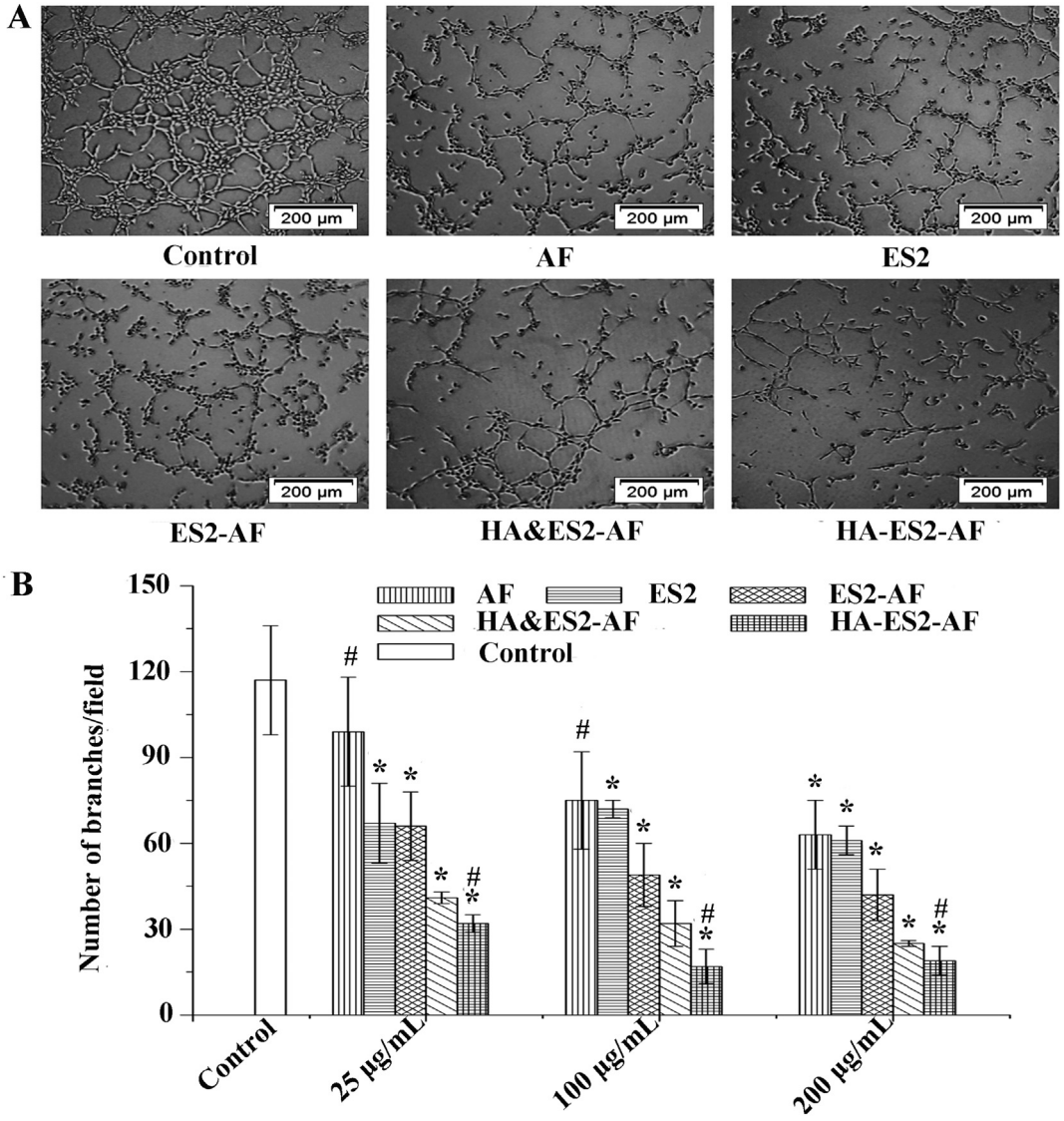

Fig. 4. Inhibition of ES2-AF and HA-ES2-AF on endothelial cell tubular morphogenesis. (A) EAhy926 cells were suspended in DMEM containing different concentrations of AF, ES2, ES2-AF, HA-ES2-AF and the mixture of HA & ES2-AF at the concentration of 200 μg/mL. PBS was used as a negative control and bFGF was added to a final concentration of 5 ng/mL. After incubation at 37 °C for 8 h, vascular network formation was observed by inverted fluorescence microscope. (B) Number of branches/field with AF, ES2, ES2-AF, HA-ES2-AF and the mixture of HA & ES2-AF after incubation for 8 h at 37 °C. Data represent means ± SD ($n = 5$). $^{*}P < .05$, significantly different compared with the control group. $^{\#}P < .05$, significantly different compared with the ES2-AF group.

inhibit endothelial cell proliferation. In contrast with ES2-AF and the mixture of HA&ES2-AF, HA-ES2-AF displayed the best inhibitory activity at all concentrations tested.

3.3. Invasion assay

Transwell assay was used to determine the effect of ES2-AF and HA-ES2-AF on endothelial cell invasion. Cells that passed through the transwell basement membrane were counted to evaluate endothelial cell invasion. As shown in Fig. 3(A, B), all groups significantly inhibited the invasion of endothelial cells ($^{*}P < .05$, significantly different compared with the control group), but the HA-ES2-AF group displayed the best inhibition on cell invasion compared with ES2-AF and HA&ES2-AF groups ($^{\#}P < .05$, significantly different from the ES2-AF and HA&ES2-AF group). At the peptide concentration of 200 μg/mL, the numbers of invaded endothelial cells with AF, ES2 and ES2-AF were (229 ± 11), (254 ± 4) and (255 ± 13), respectively. At the same concentrations, the number of invaded cells with the mixture of HA & ES2-AF and HA-ES2-AF were respectively (202 ± 24) and (170 ± 7). The above results showed that three groups (AF, ES2 and ES2-AF) had a certain amount of reduction on the number of cell invasion compared with the control group. This indicated that AF, ES2 and ES2-AF all have inhibitory effects on endothelial cell invasion, but there was no significant difference among these three peptide. This result indicated that the anti-invasion activity of ES2-AF did not increase, but only maintained the original anti-invasion activity of two short peptides. Compared with the blank control group, the invaded cells in the five treatment groups were significantly decreased, indicating that these treatment groups have an inhibitory effect on the invasion of endothelial cells. Meanwhile, comparing the ES2-AF and HA&ES2-AF groups, the number of cells in the mixture group was significantly reduced, indicating that HA can also inhibit cell invasion. Similarly, compared the HA-ES2-AF and HA&ES2-AF groups, it was found that the binding group had a stronger ability to inhibit cell invasion, which indicated that HA-modified ES2-AF significantly increased the ability of ES2-AF to inhibit cell invasion.

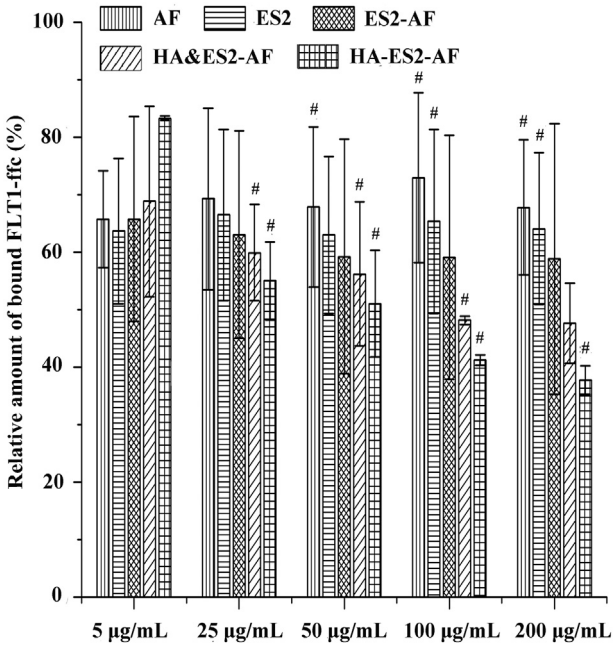

Fig. 5. The ability to inhibit the binding of VEGFR1 to $VEGF_{165}$ was assessed by an ELISA assay. Data represent means ± SD ($n = 5$). $^{\#}P < .05$, significantly different from the ES2-AF group.

3.4. Tube formation assay

Endothelial cell tube formation is essential to angiogenesis. Therefore, the tube formation assay was used to evaluate the anti-angiogenic activity of ES2-AF and its derivatives. As shown in Fig. 4(A), bFGF induced the formation of organized tubular structures in each group. In groups treated with AF, ES2, ES2-AF, the mixture of HA & ES2-AF and HA-ES2-AF, tube formation was significantly inhibited ($^{*}P < .05$, significantly different from the control group).

The number of branches in each treatment group were calculated and compared. As shown in Fig. 4(B), at peptide concentrations of 25 μg/mL, 100 μg/mL, and 200 μg/mL, the mean branches of AF, ES2 and AF-ES2 were respectively (99 ± 19), (75 ± 17), and (63 ± 12); (67 ± 14), (72 ± 3), and (61 ± 5); and (66 ± 12), (49 ± 11), and (42 ± 9). At the same concentrations, the numbers with the mixture of HA & ES2-AF were (41 ± 2), (32 ± 8), and (25 ± 1), respectively, while those of the HA-ES2-AF were (32 ± 3), (17 ± 6) and (19 ± 5), respectively. In all groups, with the increase of concentration, the number of branches was reduced in a dose-dependent manner. As seen from the above results, with the increase of the concentration, there was no significant difference in the number of branches between AF and ES2, but the number in the ES2-AF group decreased significantly. This phenomenon indicated that ES2-AF not only retained but also enhanced the anti-angiogenesis activity of the AF or ES2 peptide. The HA-ES2-AF group had the fewest tube branches compared to ES2-AF or the mixture groups. The HA-ES2-AF group exhibited the best inhibition of cell tube formation compared to the ES2-AF group ($^{\#}P < .05$, significantly different from the ES2-AF group).

These results indicate that ES2-AF has improved anti-proliferation, anti- invasion and inhibition of tube formation abilities with *in vitro* chemical modification of HA. What causes this? As mentioned earlier, AF can specifically bind VEGF and inhibit the migration of endothelial cells and tube formation; ES2 and HA have the effect of inhibiting the proliferation and invasion of endothelial cells. Therefore, we hypothesized that the combination of HA and ES2 with AF enhanced the ability of AF to bind VEGF and inhibited the binding of VEGF and VEGFR1. Therefore, we used ELISA to detect the effect of several peptides on inhibiting the binding of VEGF and VEGFR1 receptors.

3.5. ELISA assay

The inhibitory ability of the binding of VEGFR1 to $VEGF_{165}$ was assessed by an ELISA assay. $VEGF_{165}$ was coated on 96-well plates, washed to remove unbound VEGF, and then treated with each drug group. The absorbance of each treated well was measured by the TMB colouring method. The absorbance value of the positive control group was set to 100%, and the other treatment groups were statistically analysed according to the ratio of the absorbance to the control group. As shown in Fig. 5, at the peptide concentrations of 5 μg/mL, 25 μg/mL, 50 μg/mL, 100 μg/mL and 200 μg/mL, the relative amounts of AF, ES2 and ES2-AF bound to Fltl-Fc were respectively (65.74 ± 8.45)%, (69.28 ± 15.78)%, (67.86 ± 13.91)%, (72.91 ± 14.76)%, and (67.77 ± 11.75)%; (63.65 ± 12.64)%, (66.46 ± 14.87)%, (62.98 ± 13.66)%, (65.33 ± 16.01)%, and (64.08 ± 13.17)%; and (67.76 ± 17.80)%, (63.07 ± 18.05)%, (59.25 ± 20.37)%, (59.07 ± 21.25)%, and (58.84 ± 23.54)%. At the same concentrations, the amounts of Fltl-Fc bound to the mixture of HA & ES2-AF and HA-ES2-AF were (68.82 ± 16.55)%, (59.92 ± 8.35)%, (56.23 ± 12.52)%, (48.16 ± 0.72)%, and (47.65 ± 7.00)%; and (83.24 ± 0.40)%, (55.01 ± 6.81)%, (51.04 ± 9.29)%, (41.25 ± 0.92)%, and (37.76 ± 2.52)%, respectively. From the above results, it can be seen that there was no significant difference among the AF, ES2 and ES2-AF groups at the low concentrations of 5 μg/mL and 25 μg/mL. With the increase of concentration, the ES2 and ES2-AF groups showed higher inhibitory ability than the AF group, and the inhibitory ability of the ES2-AF group was slightly better than that of the ES2 group. This result indicated that ES2-AF not only retained but also enhanced the biological activity of the AF and ES2 peptides. At the same time, we found that with the increase in concentration, the inhibitory capacity of each treatment group increased in a concentration-dependent manner. We found that the inhibitory ability of the HA-ES2-AF group was significantly higher than that of the ES2-AF group ($^{\#}P < .05$, significantly different from the ES2-AF group). These results were in accordance with the hypothesis mentioned above about the improved binding ability of AF to VEGF.

3.6. CAM assay

Anti-angiogenesis effects of ES2-AF and its derivatives were tested with a classical chicken chorioallantoic membrane (CAM) assay. bFGF was added as an inducing factor for angiogenesis; thus, the effect of neovascularization was more obvious in the experimental results. As shown in Fig. 6(A), compared with the control group, the AF group showed no significant decrease in CAM neovascularization. The ES2 and ES2-AF groups inhibited neovascularization to some extent at the range of 5 μg/mL~50 μg/mL ($^{*}P < .05$, significantly different from the control group), and the activity of ES2-AF was better than that of ES2. As shown in Fig. 6(B), the degrees of angiogenesis were significantly lower in all groups than in the blank control group ($^{*}P < .05$, significantly different from the control group), and there was no significant difference between the AF group and the blank control. When the dosage was 5 μg/mL, 25 μg/mL, or 50 μg/mL and the incubation time was 24 h, the number of blood vessels in the AF, ES2 and ES2-AF groups was respectively (44.44 ± 3.04), (48.42 ± 3.90), and (42.10 ± 10.00); (39.33 ± 1.00), (28.21 ± 2.00), and (27.31 ± 6.00); and (32.03 ± 10.00), (22.84 ± 19.00), and (19.26 ± 3.00). At the same concentrations, the number of blood vessels in the mixture and HA-ES2-AF groups was (34.10 ± 3.00), (22.92 ± 2.00), and (18.58 ± 5.00); and (9.67 ± 3.00), (10.12 ± 1.00), and (13.10 ± 4.00), respectively. The above results suggest that AF has no significant inhibitory effect on CAM angiogenesis at the experimental dose. ES2-AF exhibits higher anti-angiogenic activity than ES2 *in vivo*, and anti-angiogenic activity in a dose-dependent manner. In addition, compared to ES2-AF, the mixture and HA-ES2-AF groups, we found that the three treatment groups could

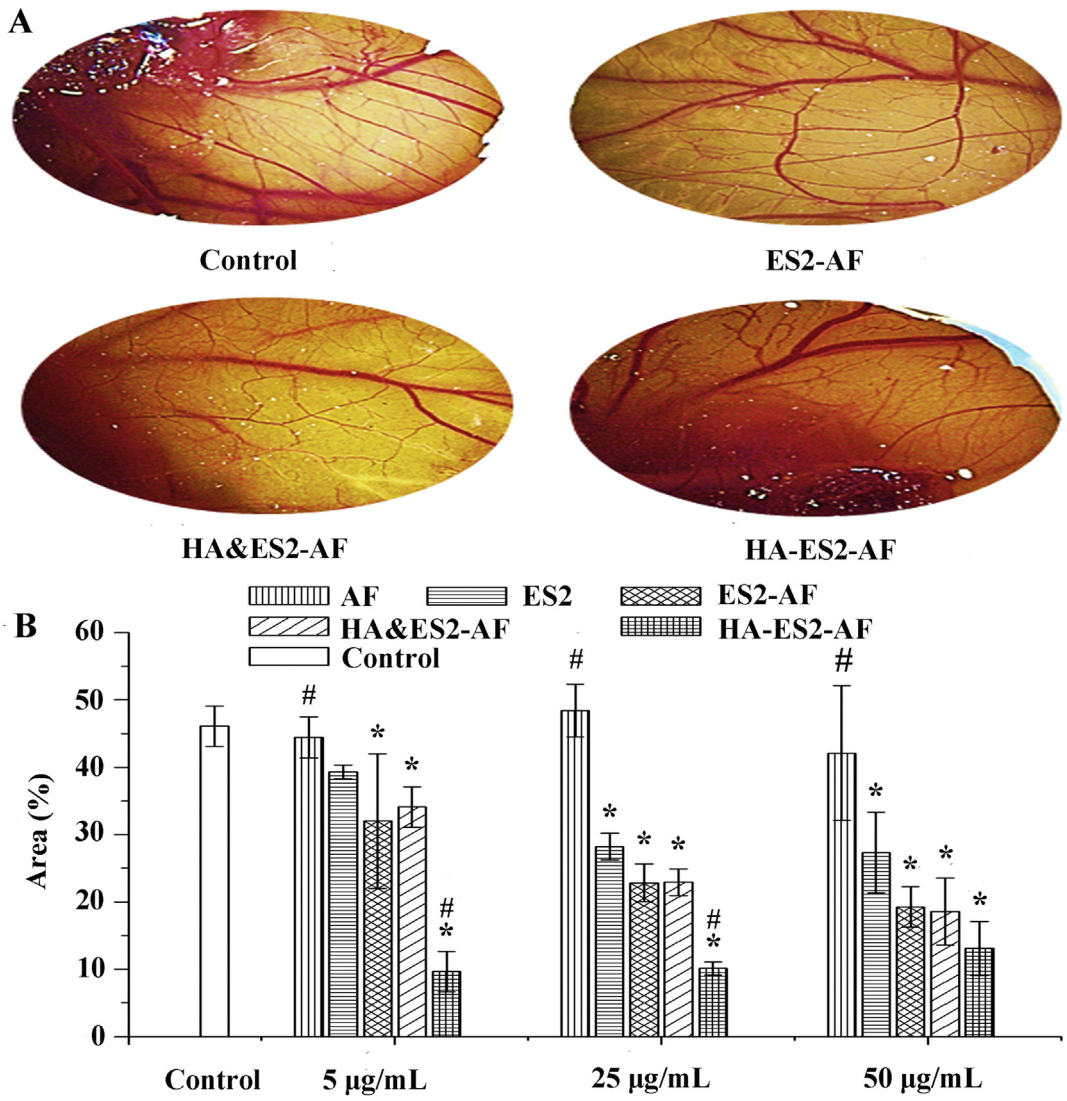

Fig. 6. Inhibition of angiogenesis with HA-ES2-AF *in vivo*. (A) Inhibition of CAM angiogenesis after incubation with AF, ES2, ES2-AF, HA-ES2-AF and the mixture of HA & ES2-AF at the concentration of 50 μg/mL (×4). (B) Comparison of the number of vessels in the AF, ES2, ES2-AF, HA-ES2-AF and the mixture of HA & ES2-AF groups after incubation for 48 h at the concentration of 5 μg/mL, 25 μg/mL and 50 μg/mL in the CAM model. Data represent means ± SD ($n = 5$). $^{*}P < .05$, significantly different from the control group. $^{\#}P < .05$, significantly different from the ES2-AF group.

significantly inhibit neovascularization, and the HA-ES2-AF group showed stronger anti-angiogenesis ability than the ES2-AF group ($^{\#}P < .05$, significantly different from the ES2-AF group). These results showed that the inhibition of CAM was improved by using HA-modified ES2-AF compared with ES-AF.

Because of the protection of the HA shell, the stability and half-life of HA-ES2-AF was thought to be better than that of ES2-AF. Thus, the bioactivity of HA-ES2-AF was much better than that of ES2-AF *in vivo*, while the bioactivity of HA-ES2-AF *in vitro* just displays slightly better activity than that of ES2-AF. In the following results, the half-life prolongation will be proven.

3.7. Pharmacokinetic study

We investigated the pharmacokinetic behaviour of ES2-AF and HA-ES2-AF in Wistar rats. The pharmacokinetic concentration-time curves after single intravenous administration of ES2-AF and HA-ES2-AF conjugate in mice are presented in Fig. 7(A). Pharmacokinetic parameters are summarized in Table 1. These data provided a clear distinction between the ES2-AF and HA-conjugated ES2-AF. The half-life time of the conjugate was prolonged from 18.07 h to 2.79 h after modification and the area under the curve (AUC) was increased 3.7 times, which could be explained by a reduction of glomerular filtration in the kidney caused by the increasing hydrodynamic radius of the peptide after attaching the HA polymer chains. These results proved that the conjugation of ES2-AF with HA improved the pharmacokinetic profiles of ES2-AF in mice. The half-life prolongation provided strong evidence for why HA-ES2-AF displays much better anti-angiogenesis activity in the CAM model. The result also provided a support for the formation of self-assembled nanoparticles/micelle-like structures.

3.8. SPR assay

To effectively determine the binding activity of CD44, a sensitive *in vitro* assay of CD44 binding has been implemented [42]. The SPR assay can be used to access the affinity of HA-ES2-AF for a CD44-coated surface. First, the preconcentration and coupling experiments of ligand protein CD44 were carried out, and the pH that was most suitable for coupling experiments was identified as 3.8 (Fig. 8A). The CD44 protein (pH = 3.8) was coupled to the ligand by the pre-set guidance function in the Biacore T200 control software to determine that the final coupling amount of the protein was 3920.7 RU. As shown in Fig. 8(B, C, D),

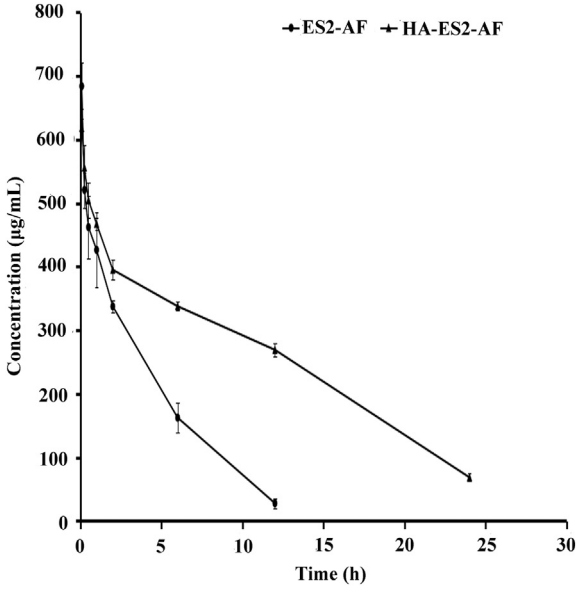

Fig. 7. Pharmacokinetic-time curves of ES2-AF and HA-ES2-AF in plasma after single intravenous administration. The results are shown as the means ± SD ($n = 5$).

Table 1
Pharmacokinetic parameters of plasma concentration of ES2-AF and HA-ES2-AF in mice.

Parameters	ES2-AF	HA-ES2-AF
Cmax (μg/mL)	684.100	618.360
$t_{1/2}$ (h)	2.785	18.070
AUC (mg/L*h)	2887.795	10,694.702
Tmax (h)	4.680	13.175

Abbreviations: $t_{1/2}$, half-life of ES2-AF and HA-ES2-AF in plasma; T_{max}, the time to reach maximum plasma concentration; C_{max}, the maximum plasma concentration of ES2-AF and HA-ES2-AF; AUC, area under the curve for the plasma concentration *versus* time curve of ES2-AF and HA-ES2-AF. Mice received a single intravenous injection of ES2-AF or HA-ES2-AF, with a dose of SOD at 25 mg/kg. The results are shown as the means ± SD ($n = 5$).

we determined the kinetic parameters of different analytes over a chip with immobilized CD44. K_D is an important parameter to measure affinity between receptor and ligand; a high K_D value indicates reduced binding. As shown in Table 2, HA as a positive control showed a low K_D value (4.198×10^{-11} mol / L); HA-ES2-AF (4.779×10^{-10} mol / L) was slightly higher than HA, and ES2-AF (3.011×10^{-4} mol / L) had a very high K_D value. Thus, after modification with HA, the affinity to CD44 of the ES2-AF conjugate was strongly improved. The CD44-binding ability of HA might give the conjugate excellent affinity for CD44. As halation significantly improved the interaction of CD44 *in vitro*, we next investigated its targeting *in vivo* using bioimaging techniques.

3.9. Bioimaging of HA-ES2-AF on tumour tissue

The ES2-AF-FITC and HA-ES2-AF-FITC conjugates were prepared as described above [25]. We also set up HA&HA-ES2-AF-FITC group separately to prove the targeting effect of HA. Nude mice bearing melanoma (B16) were randomly divided into three groups. ES2-AF-FITC, HA-ES2-AF-FITC and HA&HA-ES2-AF-FITC were injected through tail veins of the nude mice when the tumour volume became 200 mm^3. Nude mice were anaesthetized with chloral hydrate and photographed using live image system when they were in a coma; the live images were recorded at different time points after intravenous injection.

As shown in Fig. 9 (tumour was indicated using blue cycle), ES2-AF-FITC was mainly distributed in the vicinity of cervical lymph nodes after intravenous administration for 2 h, HA-ES2-AF-FITC was mainly distributed in the abdominal and cervical lymph nodes, and a small amount of fluorescence appeared at the tumour site. At the same time, the fluorescence distribution of HA&HA-ES2-AF-FITC was similar to HA-ES2-AF-FITC, mainly in the cervical lymph nodes and a small amount was distributed in the tumour site. After intravenous administration for 4 h, ES2-AF-FITC had a small amount of fluorescence signal at the tumour and bladder. Combined with the FITC metabolic pathway, we found that part of the ES2-AF-FITC was hydrolysed and discharged in the form of urine. At the same time, it was found that HA-ES2-AF-FITC began to accumulate in the tumour site. While HA&HA-ES2-AF-FITC was not found to aggregate at the tumour site, but only a small increase in fluorescence intensity was observed when compared with 2 h. After intravenous administration for 8 h, ES2-AF-FITC was concentrated in the kidney region, indicating that most of the ES2-AF-FITC had been metabolized. At this time, the intensity and area of fluorescence signals of HA-ES2-AF-FITC at the tumour site were obviously enhanced. Similarly, the fluorescence intensity of HA&HA-ES2-AF-FITC at the tumour site was only slightly increased compared with the previous time point. After intravenous administration for 12 h, the intensity and area of fluorescence signals of HA-ES2-AF-FITC and HA&HA-ES2-AF-FITC at the tumour site were obviously decreased, and a small amount of fluorescence was found in the bladder region, indicating that a small amount of metabolism began in both drugs. After intravenous administration for 24 h, HA-ES2-AF-FITC was still present in the tumour and cervical lymph nodes, and there was also a large area of fluorescence at the bladder site, indicating that 24 h later, metabolized drugs remained. As seen from the above results, the metabolic rate of HA-ES2-AF-FITC in nude mice was slower than that of ES2-AF-FITC, and the HA-modified ES2-AF had a longer plasma half-life in nude mice and was not be easily hydrolysed. At the same time, through the quantitative analysis of Fig. 9B, we also found that the fluorescence intensity of HA&HA-ES2-AF-FITC in the tumour site was significantly weaker than that of HA-ES2-AF-FITC at the same time point. The reason for this phenomenon may be that free HA can specifically bind to CD44 at the tumour site, resulting in less binding of HA to CD44 in HA-ES2-AF-FITC, thus causing the fluorescence intensity and area of the mixture group at different time points were weaker than that of HA-ES2-AF-FITC group. This result also proves the role of HA as a targeting carrier throughout the conjugate. During the whole experiment, the distribution and maintenance time of HA-ES2-AF-FITC in the tumour site was more than that of ES2-AF-FITC, indicating that HA-ES2-AF-FITC distribution targeting to tumour was better than that of ES2-AF-FITC. These findings may due to the increased stability of HA-ES2-AF in plasma and are consistent with the prolonged half-life *in vivo* from the pharmacokinetic study.

The conjugation of drug to PEG will increase the half-life, but no effects on the drug targeting can be found. In our study, the widely used drug delivery polymer HA was used to replace PEG as the modifier. We hypothesized that the conjugation of HA would not only increase the half-life but will also improve the targeting of HA-peptide conjugates to tumour tissue. The SPR assay and bioimaging assay results all support this theory. The high affinity of HA-ES2-AF for CD44 and the obviously improved targeting to tumour tissue *in vivo* make HA-ES2-AF a potential targeted anti-tumour drug.

3.10. In vivo antitumor efficiency evaluation

Antitumor activity was evaluated using B16 tumour-bearing mice. It was clear to observe that the tumors of ES2-AF group still grew with a retarded rate as compared to the s control, while the tumour growth was severely suppressed after treated with HA-ES2-AF ($P < .05$ *vs* ES2-AF) (Fig. 10A and B). The tumour growth inhibition rates of ES2-AF and HA-ES2-AF were 30.32% and 51.15% compared with the saline control.

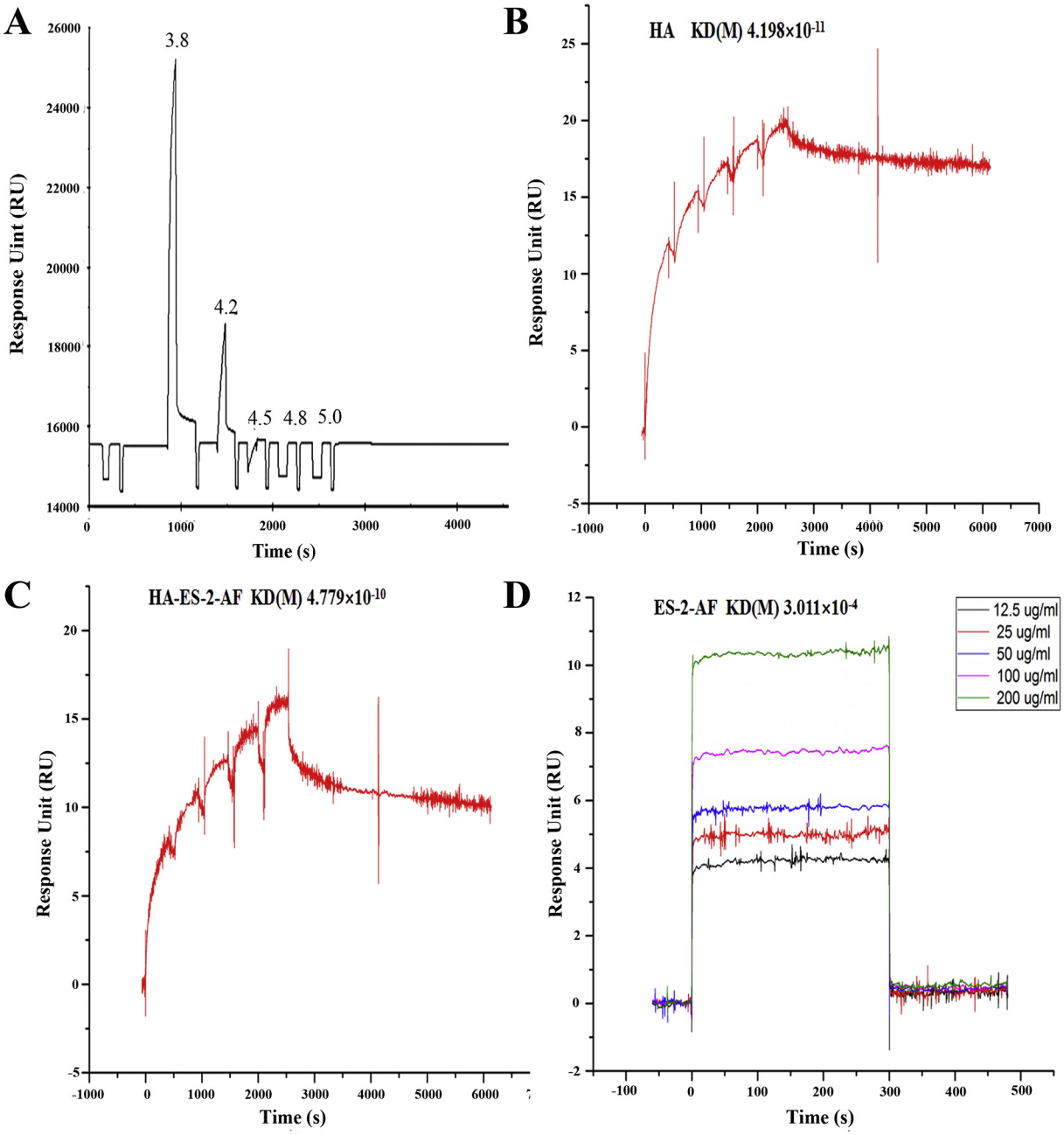

Fig. 8. Screening the optimum pH for coupling experiments and SPR sensorgram on immobilized CD44 chips from different concentrations of analytes. (A) pH scouting of CD44 in acetate buffer solution. (B) SPR sensorgram obtained from HA with different concentrations over a chip with immobilized CD44. (C) SPR sensorgram obtained from HA-ES2-AF with different concentrations over a chip with immobilized CD44. (D) SPR sensorgram obtained from ES2-AF with different concentrations over a chip with immobilized CD44.

Table 2
Kinetic parameters of different analytes over a chip with immobilized CD44.

	HA	HA-ES2-AF	ES2-AF
ka ($L{\cdot}mol^{-1}{\cdot}s^{-1}$)	4.163×10^{5}	1.178×10^{5}	–
kd (s^{-1})	1.748×10^{-5}	5.629×10^{-5}	–
KD ($mol{\cdot}L^{-1}$)	4.198×10^{-11}	4.779×10^{-10}	3.011×10^{-4}

Abbreviations: ka, binding constant; kd, dissociation constant; KD, equilibrium dissociation constant. The results are shown as the means ± SD (n = 5).

In addition, the variation of the relative body weights of the mice was shown in Fig. 10C. Body weights of the mice in HA-ES2-AF group exhibited no serious body weights reduction during the treatment, indicating no obvious systemic toxicity of HA-ES2-AF was detected. These results suggested the HA-ES2-AF possessed the most effective antitumor activity with no obvious systemic toxicity against melanoma.

3.11. Cell affinity assay

To evaluate the affinity of HA-ES2-AF to endothelial cells, FITC-labelled HA-ES2-AF and ES2-AF were respectively cultured with EAhy926 cells for 4 h. The results were shown in Fig. 11, at concentrations of 0.5 μg/mL, 1 μg/mL, 2 μg/mL, 5 μg/mL, 10 μg/mL, 25 μg/mL (concentrations of 0.5 μg/mL, 1 μg/mL, 2 μg/mL, 5 μg/mL, 10 μg/mL and 25 μg/mL pointed to the ES2-AF part only), the affinity rate of ES2-AF and endothelial cells was (4.55 ± 0.61)%, (22.79 ± 5.20)%, (82.99 ± 3.99)%, (99.61 ± 0.62)%,

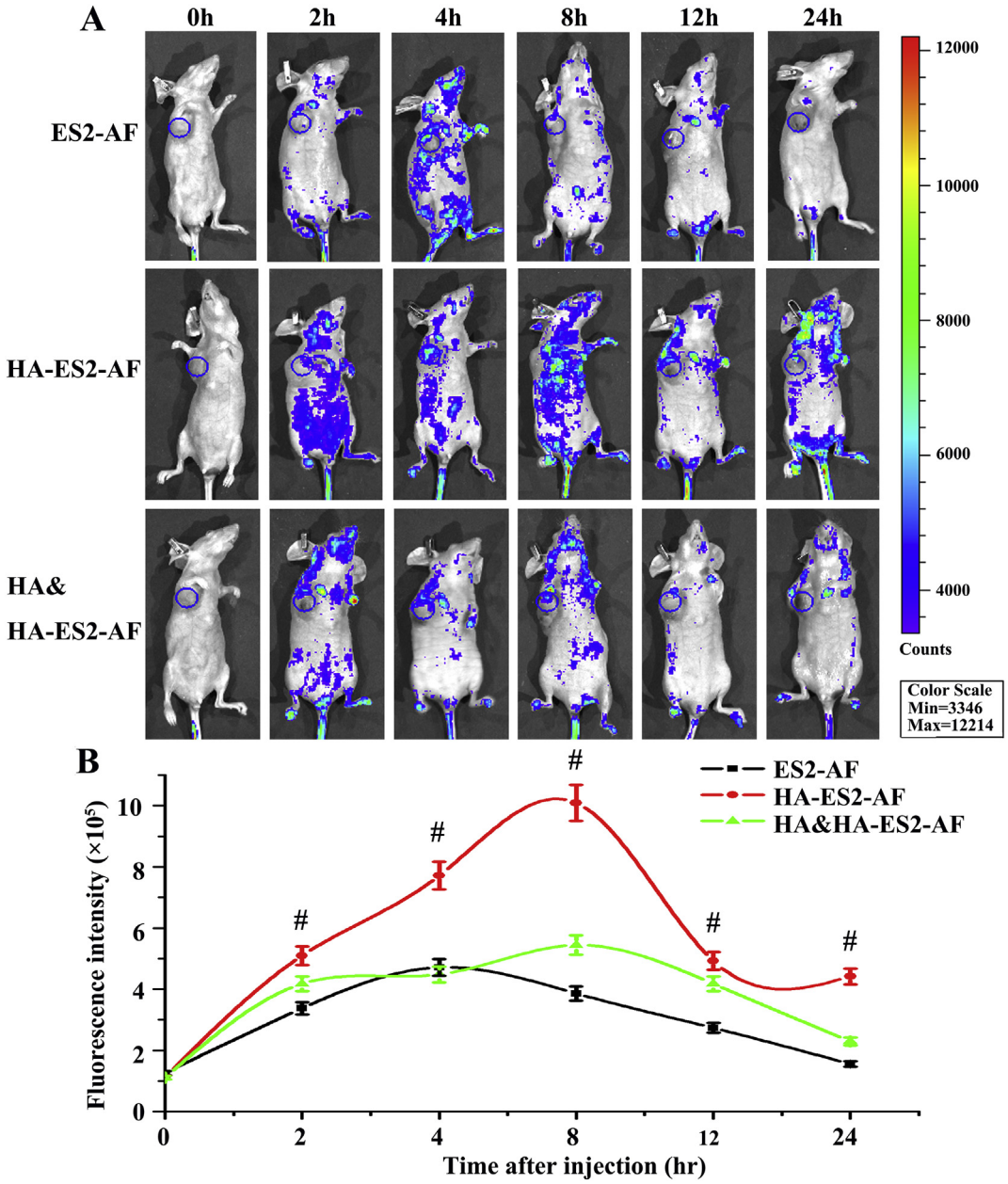

Fig. 9. *In vivo* tumour-targeting ability of HA-ES2-AF in nude mice bearing B16 tumour xenografts monitored by the Optix system. Tumour was indicated using blue cycle. (A) *In vivo* whole-body images after 0-, 2-, 4-, 8-, 12- and 24-h. (B) Quantification of fluorescence signal intensity in mice after administration of FITC-labelled ES2-AF, HA-ES2-AF and HA&HA-ES2-AF. $^{\#}P < .05$, significantly different from the ES2-AF and HA&HA-ES2-AF groups. (For interpretation of the references to colour in this figure legend, the reader is referred to the web version of this article.)

(99.63 ± 0.06)% and (99.96 ± 0.01)%, respectively. At the same concentrations, the affinity rate of HA-ES2-AF and HA&HA-ES2-AF were respectively (74.31 ± 4.95)%, (94.59 ± 3.28)%, (99.85 ± 0.01)%, (99.97 ± 0.01)%, (99.99 ± 0.01)%, (99.96 ± 0.02)% and (20.01 ± 1.99)%, (75.83 ± 5.08)%, (97.98 ± 0.34)%, (99.88 ± 0.12)%, (99.98 ± 0.02)%, (99.98 ± 0.02)%. From the above results, when the concentration was lower than 5 μg/mL, the affinity activity of HA-ES2-AF and ES2-AF was significantly different, indicating that the modification of HA significantly increased the affinity of ES2-AF for endothelial cells. To verify this conjecture, we added free HA to see if it could competitively inhibited the binding ability of HA-ES2-AF to endothelial cells. The results showed that the affinity rate of HA&HA-ES2-AF group was significantly lower than the HA-ES2-AF group at this concentration, indicating that the combination of free HA to endothelial cells competitively inhibited the binding of HA-ES2-AF to endothelial cells. As can be seen from the figure, when the concentration was higher than 5 μg/mL, the affinity of the peptides and conjugates to endothelial cells was all close to 100%, indicating that the presence of AF structure in ES2-AF made the affinity of both ES2-AF and HA-ES2-AF to a high level. This result echoes the results of bioimaging and *in vivo* antitumor experiments, further explaining why the modification of HA allows ES2-AF to have better targeting and antitumor activity *in vivo*.

4. Conclusion

To conclude, ES2-AF was synthesized by a solid-phase method in this study, and HA-ES2-AF was obtained by HA chemical modification of the new peptide ES2-AF. First, ^{1}H NMR spectroscopy showed that HA successfully bound to ES2-AF and that there were 60 peptides per 1 HA chain.

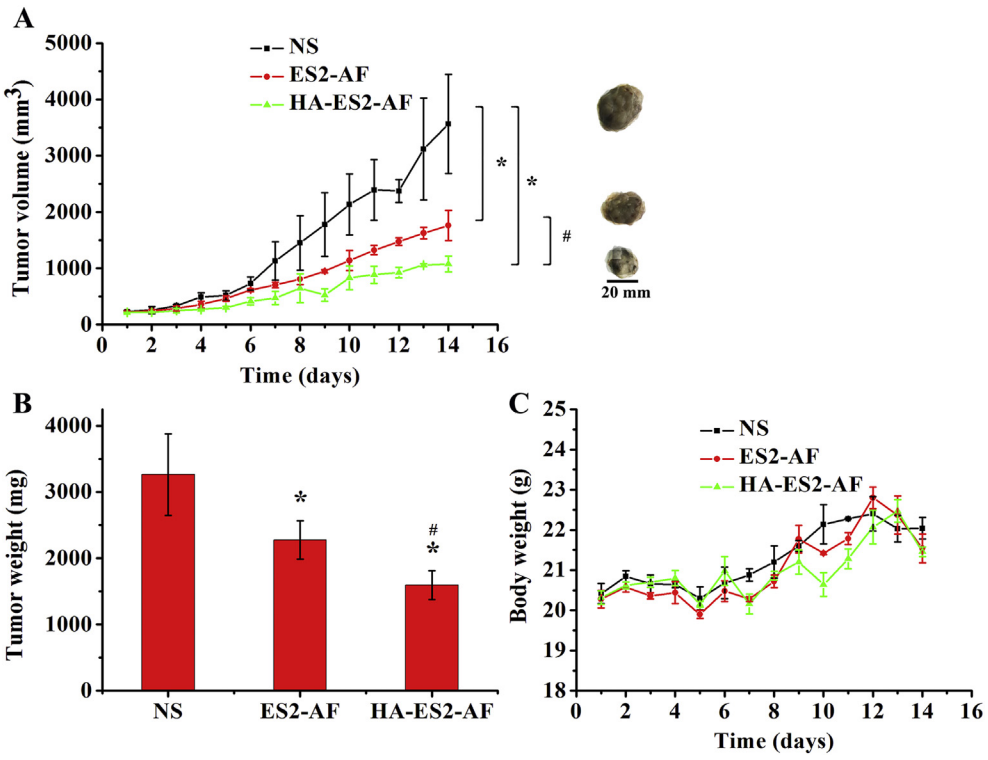

Fig. 10. *In vivo* antitumor efficacy of ES2-AF and HA-ES2-AF on B16 tumour-bearing mice. (A) Tumour volume-time graph. (B) Variation of tumour weight. (C) Body weight change of each treatment group. Data represent means ± SD ($n = 5$). $^{*}P < .05$, significantly different from the NS group. $^{\#}P < .05$, significantly different from the ES2-AF group.

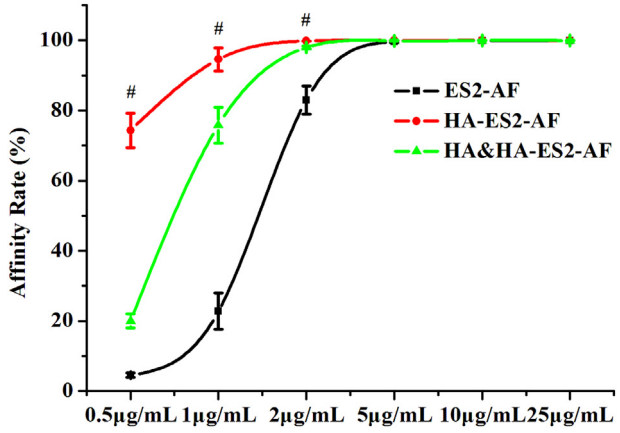

Fig. 11. Affinity efficacy of ES2-AF and HA-ES2-AF on endothelial cells. Data represent means ± SD ($n = 5$). $^{\#}P < .05$, significantly different from the ES2-AF group.

We then performed *in vitro* studies on the activity of ES2, ES2-AF and HA-ES2-AF. HA-ES2-AF was found to have a strong inhibitory effect on the proliferation of endothelial cells; ES2-AF inhibited the proliferation of endothelial cells, in contrast to ES2 and was concentration-dependent. In terms of anti-invasion of endothelial cells and inhibition of tube formation, we found that the inhibitory effect of HA-ES2-AF was more pronounced than that of ES2-AF. However, ES2-AF inhibited endothelial cell tube formation more strongly than did ES2 and AF, but its anti-invasion ability was similar to that of ES2 and AF. These results indicate that ES2 and HA inhibit the proliferation and invasion of endothelial cells. Next, we used ELISA to detect the effect of several peptides in inhibiting the binding of VEGF and VEGFR1 receptors. Surprisingly, it was found that the inhibitory rate of a high concentration of HA-ES2-AF was higher than that of ES2-AF; ES2-AF had stronger inhibitory activity than AF. At the same time, because HA can specifically bind to CD44, we used surface plasmon resonance analysis to study the interaction of ES2-AF and HA-ES2-AF with CD44 protein. The results showed that the affinity of HA-ES2-AF for CD44 protein was slightly lower than that of HA; however, compared with ES2-AF, its affinity activity was greatly improved.

Through a bioimaging study *in vivo*, it was found that the distribution of HA-ES2-AF in tumour sites was significantly enhanced compared with ES2-AF. This is consistent with our previous conjecture. After binding of ES2-AF to HA, we used the characteristics of HA specifically binding to CD44 and as a carrier of ES2-AF to deliver ES2-AF to tumors, thus compensating for the poor targeting of ES2-AF. The conclusion that HA-ES2-AF better inhibits tumour growth *in vivo* also proves this conclusion.

In addition, in bioimaging results we found that HA-ES2-AF had a longer metabolic time compared to ES2-AF *in vivo*, which may due to the increased stability of HA-ES2-AF in plasma. That was consistent with the *in vivo* half-life experiments. The half-life of HA-ES2-AF was approximately 6-fold longer than that of ES2-AF. These data strongly suggest that hyaluronic acid has the desired effect of extending the half-life of this peptide drug.

In conclusion, ES2-AF that has been modified by HA has increased anti-neovascularization activity *in vitro* and *in vivo*, higher targeting to tumour tissue, significantly prolonged half-life *in vivo*, and thus has better anti-tumour activity *in vivo*, providing the foundation for its further development as a targeted anti-tumour drug.

Author contributions

The manuscript was written through contributions of all authors. All authors have given approval to the final version of the manuscript.

Acknowledgements

This work was supported by National Natural Science Foundation of China (81473129), Shandong Provincial Key Research and Development Program (2015GSF118099) and The Fundamental Research Funds of Shandong University (2014JC044).

References

[1] J. Folkman, Anti-angiogenesis: new concept for therapy of solid tumors, Ann. Surg. 175 (1972) 409–416.
[2] J. Folkman, Antiangiogenesis in cancer therapy—endostatin and its mechanisms of action, Exp. Cell Res. 312 (2006) 594–607.
[3] J. Folkman, K. Watson, D. Ingber, D. Hanahan, Induction of angiogenesis during the transition from hyperplasia to neoplasia, Nature 339 (1989) 58–61.
[4] L.H. Xu, H.N. Tan, F.S. Wang, W. Tang, Research advances of endostatin and its short internal fragments, Curr. Protein Pept. Sci. 9 (2008) 275–283.
[5] R.M.T.T. Tjin, R. Satchi-Fainaro, A.E. Birsner, V. Ramanujam, J. Folkman, K. Javaherian, A 27-Amino-Acid synthetic peptide corresponding to the NH2-terminal zinc-binding domain of endostatin is responsible for its antitumor activity, Cancer Res. 65 (2005) 3656–3663.
[6] S.A. Wickstrom, K. Alitalo, J. Keski-Oja, An endostatin-derived peptide interacts with integrins and regulates actin cytoskeleton and migration of endothelial cells, J. Biol. Chem. 279 (2004) 20178–20185.
[7] Z. Qiu, J.L. Hu, H.M. Xu, W.J. Wang, C.H. Nie, X. Wang, Generation of antitumor peptides by connection of matrix metalloproteinase-9 peptide inhibitor to an endostatin fragment, Anti-Cancer Drugs 24 (2013) 677–689.
[8] Y.Y. Wan, G.Y. Tian, H.S. Guo, Y.M. Kang, Z.H. Yao, X.L. Li, Q.H. Liu, D.J. Lin, Endostatin, an angiogenesis inhibitor,ameliorates bleomycin-induced pulmonary fibrosis in rats, Respir. Res. 14 (2013) 56.
[9] X.Y. Huang, X.M. Zhang, F.H. Chen, L.L. Zhou, X.F. Deng, Y.J. Liu, X.J. Li, Anti-proliferative effect of recombinant human endostatin on synovial fibroblasts in rats with adjuvant arthritis, Eur. J. Pharmacol. 723 (2014) 7–14.
[10] L. Zheng, D.M. Zhang, X.C. Chen, L. Yang, Y.Q. Wei, X. Zhao, Antitumor activities of human placenta-derived mesenchymal stem cells expressing endostatin on ovarian cancer, PLoS One 7 (2012) e39119.
[11] E.J. Oh, J.S. Choi, H. Kim, C.K. Joo, S.K. Hahn, Anti-Flt1 peptide–hyaluronate conjugate for the treatment of retinal neovascularization and diabetic retinopathy, Biomaterials 32 (2011) 3115–3123.
[12] E.J. Oh, K. Park, J.S. Choi, C.K. Joo, S.K. Hahn, Synthesis, characterization, and preliminary assessment of anti-Flt1 peptide–hyaluronate conjugate for the treatment of corneal neovascularization, Biomaterials 30 (2009) 6026–6034.
[13] T. Suganuma, K. Ino, K. Shibata, H. Kajiyama, T. Nagasaka, S. Mizutani, F. Kikkawa, Functional expression of the angiotensin II type1 receptor in human ovarian carcinoma cells and its blockade therapy resulting in suppression of tumor invasion, angiogenesis, and peritoneal dissemination, Clin. Cancer Res. 11 (2005) 2686–2694.
[14] D. Schumacher, C.P.R. Hackenberger, More than add-on: chemoselective reactions for the synthesis of functional peptides and proteins, Curr. Opin. Chem. Biol. 22 (2014) 62–69.
[15] G. Pasut, F.M. Veronese, State of the art in PEGylation: the great versatility achieved after forty years of research, J. Control. Release 161 (2012) 461–472.
[16] J.K. Armstrong, G. Hempel, S. Koling, L.S. Chan, T. Fisher, H.J. Meiselman, G. Garratty, Antibody against poly (ethylene glycol) adversely affects PEG-asparaginase therapy in acute lymphoblastic leukemia patients, Cancer 110 (2007) 103–111.
[17] M.R. Sherman, M.G.P. Saifer, F. Perez-Ruiz, PEG-uricase in the management of treatment-resistant gout and hyperuricemia, Adv. Drug Deliv. Rev. 60 (2008) 59–68.
[18] C.E. Schanté, G. Zuber, C. Herlin, T.F. Vandamme, Chemical modifications of hyaluronic acid for the synthesis of derivatives for a broad range of biomedical applications, Carbohydr. Polym. 85 (2011) 469–489.
[19] R. Stern, A.A. Asari, K.N. Sugahara, Hyaluronan fragments: an information-rich system, Eur. J. Cell Biol. 85 (2006) 699–715.
[20] M. Slevin, J. Krupinski, J. Gaffney, S. Matou, D. West, H. Delisser, R.C. Savani, S. Kumar, Hyaluronan-mediated angiogenesis in vascular disease: uncovering RHAMM and CD44 receptor signaling pathways, Matrix Biol. 26 (2007) 58–68.
[21] A. Mero, M. Pasqualin, M. Campisi, D. Renier, G. Pasut, Conjugation of hyaluronan to proteins, Carbohydr. Polym. 92 (2013) 2163–2170.
[22] W.M. Gramlich, I.L. Kim, J.A. Burdick, Synthesis and orthogonal photopatterning of hyaluronic acid hydrogels with thiol-norbornene chemistry, Biomaterials 34 (2013) 9803–9811.
[23] H. Kim, J.S. Choi, K.S. Kim, J.A. Yang, C.K. Joo, S.K. Hahn, Flt1 peptide–hyaluronate conjugate micelle-like nanoparticles encapsulating genistein for the treatment of ocular neovascularization, Acta Biomater. 8 (2012) 3932–3940.
[24] F.F. Chen, Y. Liu, F. Wang, X.J. Pang, C.D. Zhu, M. Xu, W. Yu, X.J. Li, Effects of upregulation of Id3 in human lung adenocarcinoma cells on proliferation, apoptosis, mobility and tumorigenicity, Cancer Gene Ther. 22 (2015) 431–437.
[25] Y. Yu, F. Sun, C.C. Zhang, Z.D. Wang, J.F. Liu, H.N. Tan, Study on glyco-modification of endostatin-derived synthetic peptide endostatin2 (ES2) by soluble chitooligosaccharide, Carbohydr. Polym. 154 (2016) 204–213.
[26] X.Y. Huang, X.M. Zhang, F.H. Chen, L.L. Zhou, X.F. Deng, Y.J. Liu, X.J. Li, Anti-proliferative effect of recombinant human endostatin on synovial fibroblasts in rats with adjuvant arthritis, Eur. J. Pharmacol. 723 (2014) 7–14.
[27] D.S. Liang, H.T. Su, Y.J. Liu, A.T. Wang, X.R. Qi, Tumor-specific penetrating peptides-functionalized hyaluronic acid-d-α-tocopheryl succinate based nanoparticles for multi-task delivery to invasive cancers, Biomaterials 71 (2015) 11–23.
[28] L. Guo, N. Song, T. He, F. Qi, S. Zheng, Endostatin inhibits the tumorigenesis of hemangioendothelioma via downregulation of CXCL1, Mol. Carcinog. 54 (2015) 1340–1353.
[29] Y. Bai, M. Zhao, C. F. Zhang, S. S. Li, Y. Qi, B, Wang, L. Z. Hang, X. X. Li, Anti-angiogenic effects of a mutant endostatin: a new prospect for treating retinal and choroidal neovascularization, PLoS One 9 (2014) e112448.
[30] X.M. Xu, W. Mao, Q. Chen, Q. Zhuang, L.H. Wang, J. Dai, H.B. Wang, Z.Q. Huang, Endostar, a modified recombinant human endostatin, suppresses angiogenesis through inhibition of Wnt/β-catenin signaling pathway, PLoS One 9 (2014) e107463.
[31] Z.H. Ren, Y.N. Wang, W.H. Jiang, W. Dai, Y.P. Jiang, Anti-tumor effect of a novel soluble recombinant human endostatin: administered as a single agent or in combination with chemotherapy agents in mouse tumor models, PLoS One 9 (2014) e107823.
[32] E.J. Oh, K. Park, K.S. Kim, J. Kim, J.A. Yang, J.H. Kong, M.Y. Lee, A.S. Hoffman, S.K. Hahn, Target specific and long-acting delivery of protein, peptide, and nucleotide therapeutics using hyaluronic acid derivatives, J. Control. Release 141 (2010) 2–12.
[33] J.J. Xue, L. Jin, X.K. Zhang, F.S. Wang, P.X. Ling, J.Z. Sheng, Impact of donor binding on polymerization catalyzed by KfoC by regulating the affinity of enzyme for acceptor, BBA-Gen. Subjects 1860 (2016) 844–855.
[34] T.L. Ying, P. Prabakaran, L.Y. Du, W. Shi, Y. Feng, Y.P. Wang, L.S. Li, W. Wang, S.B. Jiang, D.S. Dimitrov, T.Q. Zhou, Junctional and allele-specific residues are critical for MERS-CoV neutralization by an exceptionally potent germline-like antibody, Nat. Commun. 8223 (2015) 1–10.
[35] L.K. Liu, B.C. Finzel, Fragment-based identification of an inducible binding site on cell surface receptor CD44 for the design of protein–carbohydrate interaction inhibitors, J. Med. Chem. 57 (2014) 2714–2725.
[36] K.C. Park, S.H. Choi, Effects of endostatin and a new drug terpestacin against human neuroblastoma xenograft and cell lines, Pediatr. Surg. Int. 29 (2013) 1327–1340.
[37] J.A. Yang, W.H. Kong, D.K. Sung, H. Kim, T.H. Kim, K.C. Lee, S.K. Hahn, Hyaluronic acid–tumor necrosis factor-related apoptosis-inducing ligand conjugate for targeted treatment of liver fibrosis, Acta Biomater. 12 (2015) 174–182.
[38] X. Pang, X. Yang, G. Zhai, Polymer-drug conjugates: recent progress on administration routes, Expert Opin. Drug Del. 11 (2014) 1075–1086.
[39] E.M. Pelegri-Oday, E. Lin, H.D. Maynard, Therapeutic protein-polymer conjugates: advancing beyond pegylation, J. Am. Chem. Soc. 136 (2014) 14323–14332.
[40] G. Saravanakumar, V.G. Deepagan, R. Jayakumar, J.H. Park, Hyaluronic acid-based conjugates for tumor-targeted drug delivery and imaging, J. Biomed. Nanotechnol. 10 (2014) 17–31.
[41] D.C. West, S. Kumar, The effect of hyaluronate and its oligosaccharides on endothelial cell proliferation and monolayer integrity, Exp. Cell Res. 183 (1989) 179–196.
[42] P. Rooney, S. Kumar, J. Ponting, M. Wang, The role of hyaluronan in tumour neovascularization (review), Int. J. Cancer 60 (1995) 632–636.